AT&T Technical Journal
Vol. 64, No. 3, March 1985
Printed in U. S. A.

Reliability of InGaAs Photodiodes for SL Applications

By R. H. SAUL,* F. S. CHEN,* and P. W. SHUMATE, JR.†

(Manuscript received March 6, 1984)

A major objective of the TAT-8 submarine cable development program is the reliability assurance of its critical components. A relatively new device, the InGaAs photodiode, is used as the detection element in optical receivers and as the monitor of laser output in optical transmitters. In this paper, we describe a comprehensive reliability program aimed at assessing and assuring the reliability of InGaAs photodiodes. A major portion of this work has involved device operation at overstress conditions. Results to date indicate that for receiver photodiodes a device design exists which is predicted to meet a 1-FIT reliability objective. Tests of monitors of similar design are in progress. Critical to the success of the reliability assurance program is the ability to identify weak devices which are likely to fail early in the system life cycle. A conventional high-temperature burn-in is shown to be impractical, and it would not necessarily remove devices which fail by low activation energy processes. Overvoltage provides a means of accelerating such failure mechanisms. A "purge" using a combination of accelerants (high temperature and overvoltage) is shown to have considerable promise in failing weak devices, while inducing significant changes in those devices which subsequently fail early in a life test (elevated temperature at normal bias conditions). Devices which are unaffected by the purge are shown by extended life tests to be robust devices which have a high probability of meeting TAT-8 requirements.

I. INTRODUCTION

Photodiodes fabricated with an InGaAs absorbing region have high

* AT&T Bell Laboratories. † AT&T Bell Laboratories; present affiliation Bell Communications Research, Inc.

quantum efficiency over the 1.0- to 1.6-μm wavelength region. These devices are used in all long-wavelength lightwave transmission systems being developed by AT&T Bell Laboratories. The Submarine Cable (SL) application utilizes InGaAs photodiodes as the photosensitive element in receivers and as monitors of laser output for power stabilization in transmitters. The high repair costs associated with an undersea installation put great emphasis on assuring that the reliability requirement of each critical component is met. While initial reliability information on InGaAs photodiodes, either generated in the laboratory[1–3] or through our terrestrial applications,[4] led us to be optimistic about the long-term stability of these devices, it was clear that a comprehensive reliability evaluation was required. In addition, although there is extensive AT&T experience with short-wavelength (silicon) photodiodes in FT3 lightwave systems, the photodiode screening procedures for assuring reliability are not directly applicable because of substantial differences in manufacturing technologies and semiconductor properties.

The first phase of our reliability program involved substantial testing of InGaAs photodiodes under various overstress conditions of temperature, humidity, bias, etc. Coupled with failure mode analysis, this phase revealed design and fabrication flaws, whose subsequent elimination led to devices with enhanced reliability. Extensive *qualification* testing then established that the design met system reliability objectives. Since in manufacture it is expected that some devices will be flawed and will therefore be susceptible to premature failures, a *certification* process is required which "purges" out the flawed devices, leaving a surviving population of robust devices which have a high probability of meeting SL reliability objectives. A *surveillance* phase of this process involves the accelerated testing of a portion of the survivors to establish that the manufactured devices match the reliability statistics of the previously qualified devices. The remaining survivors are then incorporated into receivers or laser packages and subjected to further extended operational testing. Final selection of receivers or laser packages for undersea installation is then made. Long-term tests are continued on a portion of these packages to reveal the true reliability statistics of the manufactured population; the results help determine maintenance strategy.

Key to the success of the certification process is the development of a purge procedure. In general this procedure will include thermomechanical tests (temperature cycling, mechanical shock, vibration, hermeticity, etc.) to weed out packaged devices that have assembly flaws. Additionally, and most importantly, the photodiode chips must be operated under carefully selected overstress conditions which promote failure or cause detectable instabilities or changes in devices that

contain manufacturing flaws. It is desirable that the life of the surviving (robust) devices should not be deleteriously affected, however. The critical issue is to assure that devices which survive the purge procedure do not fail during the service life of the system. Ideally, the type of stress and the failures induced should be the same as those encountered in normal operation so that relevant failure modes are stimulated. However, a variety of stresses can be employed to eliminate all but the most robust devices. We have found that simultaneous application of high temperature and high reverse bias is a promising method for achieving the desired objectives.

In the following section we review the photodiode device design from the standpoint of reliability. Critical device parameters and potential failure modes are discussed in Section III. Results of accelerated aging tests, used to qualify the device design, are described in Section IV. The development of a purge is then discussed in Section V.

II. REVIEW OF DEVICE DESIGN: CONSIDERATIONS FOR RELIABILITY

Initial InGaAs photodiodes were fabricated in a mesa geometry.[5-7] These devices were simple to fabricate and capable of low dark currents. While stable operation has been reported for several thousand hours in limited samples,[2,3] we believe that long-term device stability is compromised in the mesa geometry since the junction perimeter is exposed. Contaminants on the mesa walls can result in surface leakage; the slow ingress of contaminants along the p-n junction can also increase generation-recombination current. Planar photodiodes, on the other hand, are more amenable to surface passivation which seals the junction and (ideally) stabilizes surface states. Figure 1 schematically illustrates the planar InGaAs photodiodes developed at AT&T Bell Laboratories.[8] Device characteristics for SL receiver and monitor applications are given in Table I. Several design features are noteworthy. Back-face illumination[6] eliminates carrier loss due to surface recombination, thus enhancing quantum efficiency. A quarter-wave SiN_x film on the substrate side provides an Antireflection (AR) coating. On the junction side of the chip a double dielectric layer is used: the first SiN_x layer serves as a mask for selected area diffusion; the second SiN_x layer defines the p-contact area and serves as an additional passivation layer which completes the sealing of the surface. The entire junction area is therefore protected from the ambient. Further, the metal contact to the semiconductor surface is restricted so that the stress, associated with the metallization-semiconductor interface, is removed from the junction perimeter. Initially, plated p-contacts were used; however, bias aging at high humidity showed a fivefold improvement in mean times to failure with e-beam evaporated

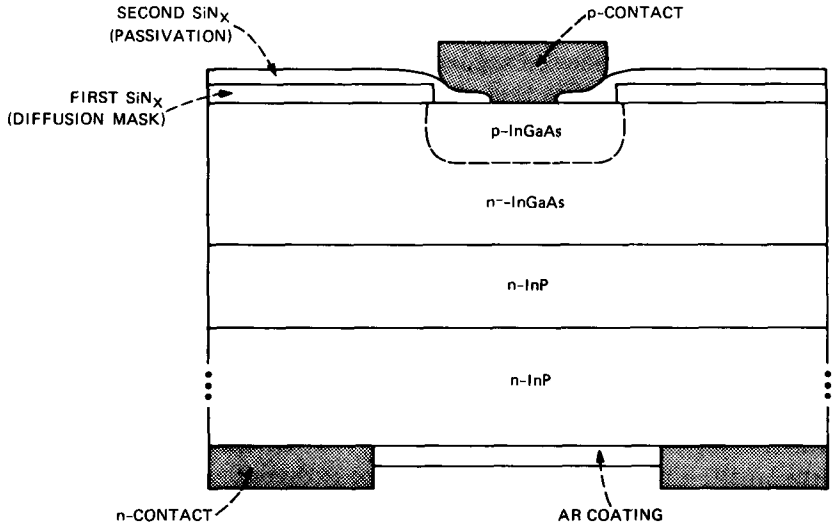

Fig. 1—Schematic illustration of planar InGaAs/InP photodiode. Typical characteristics are given in Table I.

Table I—Photodiode characteristics for SL applications

	Receiver ($V_R = 10V$)	Monitor ($V_R = 5V$)
Junction diameter (μm)	78	250
Maximum dark current (nA)	40	100
Maximum capacitance (pF)*	0.42	7.0
Minimum quantum efficiency	0.8	0.6
Maximum rise/fall time (ns)	0.5	0.5

* Chip only.

contacts.[9] The improvement is thought to be the result of reduced contamination and the absence of pores in the metallization. This design results in low dark current, high quantum efficiency, and, as shown below, excellent reliability.

III. CRITICAL DEVICE PARAMETERS AND POTENTIAL FAILURE MODES

In this section we briefly consider the device parameters which are critical to system operation, discuss possible failure modes, and suggest methods for probing sensitivity to the associated failure mechanisms. In general, increased dark current, increased capacitance, and reduced quantum efficiency deleteriously affect receiver sensitivity. Additionally, pulse rise and fall times must not increase to the point that they become comparable to the data time slot. For the monitor application, quantum efficiency and its spatial uniformity are the principal parameters. Electrical continuity is obviously critical to both applications.

Table II—Critical device parameters and potential failure mechanisms

Parameter	Potential Failure Mechanisms	Accelerants
• Dark current	Bulk leakage (junction degradation, local breakdown)	High-temperature bias Overvoltage
	Surface leakage	High humidity Thermal cycling
• Capacitance	Diffusion, doping density changes	High temperature
• Quantum efficiency	"Darkening" of InP	High temperature
	Degradation of AR coating	
• Rise/fall times	Formation of traps	High-temperature bias
• Electrical continuity	Open wire or chip bond	Thermal cycling
	Fractured chip	Centrifuge Vibration Shock

Table II summarizes, for these parameters, potential failure mechanisms and accelerants. A detailed discussion is given below.

3.1 Receiver photodiode

Failure of the photodiode in a digital lightwave receiver can impact operation of a repeater section in two ways, either through catastrophic failure or gradual degradation evidenced by a slowly increasing error rate. Catastrophic failures can occur in these devices either from opens due to die- or wire-bond failures, fractured chips, or from shorted devices. Metallization-related failure modes, viz., electrolytic corrosion and electromigration, are not expected because of the low current density and low electric field in these devices.

Gradual degradation in the detector electro-optical properties can lead to decreased receiver sensitivity. Clearly, a decrease in photodiode quantum efficiency results in a proportional decrease in sensitivity. Such degradation could, for example, arise from changes in the AR coating applied to the device. Quantum efficiency could also decrease if absorbing regions were to develop in the transparent InP substrate, or if recombination centers were to develop in the InGaAs epitaxial material.

Absorbing or recombination regions ("dark-spot" or "dark-line" defects) observed in high-radiance LEDs and lasers usually result from nonradiative recombination processes.[10] In detectors, photo-excited carriers are rapidly separated by the field in the depletion layer, i.e., there is no carrier recombination. Moreover, the current densities are several orders of magnitude lower than for LEDs and lasers. Consequently, these phenomena are not expected to occur. In fact, after 1500 hours of accelerated aging at 200°C, the observed changes in quantum efficiency of (AR-coated) photodiodes are less than ±0.1 dB. Assuming an activation energy greater than 0.5 eV (see Section 4.1), this is equivalent to $\gtrsim 2 \times 10^6$ hours of operation at TAT-8 conditions

(≤30°C). Similar findings have been reported for mesa InGaAs photodiodes.[3]

Other parameters contribute to receiver sensitivity in increasingly subtle but well-understood ways.[11] For example, the detector dark current contributes shot noise at the receiver input, degrading the signal-to-noise ratio. Consequently, the usual failure mode in photodetectors is taken as increased dark current[12] with End-Of-Life (EOL) determined by a prescribed degradation in receiver sensitivity (e.g., 1 dB). The increase in dark current can arise from either surface and/or bulk contributions. As mentioned above, poor or no passivation can lead to contamination of the junction, resulting in surface leakage. Furthermore, field-assisted migration of impurities from the surface into the diode's active region can result in increased generation-recombination current. Also, field-assisted drift of charge in the dielectric can result in inversion or accumulation on the semiconductor surface which, by increasing the depletion layer volume, would increase generation-recombination current.

The dark-current shot noise, however, is not necessarily the most important noise parameter. The dependence of the mean-squared shot-noise current on bandwidth or bit rate B (receiver bandwidth is approximately 0.5·bit rate) is linear, whereas other noise terms vary as higher powers of B. For example, for the SL receiver that uses a bipolar transistor as the first gain element, the capacitance of the detector multiplies transistor noise terms that vary as B^2 and B^3. Thus, at the SL bit rate of 296 Mb/s, dark current is not a major noise source until it reaches the order of 1 μA. As described in Section IV, we find that in accelerated aging tests, the dark current (I_d) can increase very rapidly, eventually resulting in a virtually shorted device. We have taken $I_d \geq 100$ nA as the operational definition of "end-of-life"; experimentally we find that this definition is essentially equivalent because of the catastrophic increase in I_d.

As suggested above, detector capacitance strongly influences SL receiver sensitivity and it conceivably could increase with time to reduce sensitivity. For example, thermally activated changes in the diffusion profile could alter capacitance. Since the capacitance is determined by the large width of the "intrinsic" region in a pin diode, plus relatively small depletion widths in the p and n material on either side, and since the operating temperature is only about one-third of the absolute temperature at which diffusion is performed, it is highly improbable that such changes will occur. On the other hand, charge accumulation near the surface could induce local changes in the depletion layer width. As in the case of quantum efficiency, no significant changes ($< \pm 0.02$ pF) have been observed in accelerated tests, consistent with results reported elsewhere.[3]

Finally, the intrinsic rise time of the detector can affect receiver sensitivity through Intersymbol Interference (ISI). The equalizer in the linear channel of a receiver is normally adjusted at the time of manufacture. If subsequent changes in the detector alter the pole location(s) of the receiver, the equalizer is no longer correctly compensating for these poles and intersymbol interference appears. Within the resolution of our rise-time measurement (±30 ps), no changes in this parameter have been observed after 1500 hours of accelerated aging at 200°C.

3.2 Monitor photodiodes

The discussion of the preceding section largely applies in the case of the laser monitors. Since the quantum efficiency directly scales the current level used as an analog of the laser output for control and stabilization purposes, quantum efficiency must remain stable at least to the extent that the laser output must remain stable. In present applications of these monitor detectors, capacitance and rise time play relatively unimportant roles. Dark current in the laser monitor is limited by its possible effect on the laser feedback-control circuit, being interpreted equally with true photocurrent as a "light level." The circuit-imposed limit on dark current is 5 μA, which is taken as the operational definition of end-of-life.

IV. ACCELERATED AGING TESTS

Long-term accelerated aging tests have been conducted on over 500 receiver and monitor photodiodes. These results have produced iterations in the device design for enhancing reliability and provide the basis for qualifying the device design for TAT-8. We first consider tests that utilize high temperature as a means for accelerating failure.

4.1 High temperature-bias aging

Photodiodes, assembled in hermetic packages, were operated at the normal bias condition at various elevated temperatures in the range 85 to 260°C. In situ measurements of I_d were made. Periodically, devices were cooled (while biased) to room temperature for measurements of I_d, reverse breakdown voltage V_{BR}, and, for some devices, rise and fall times, quantum efficiency, and capacitance. Figure 2 illustrates a typical I-V characteristic as a function of aging time. I_d (defined at the operating voltage) remains nearly constant, in general for an extended period, then may slowly increase, and finally increases rapidly to failure—defined as 100 nA for receiver photodiodes and 5 μA for monitor photodiodes. The slow degradation is not always present and its rate is not correlated to the onset of the rapid rise in

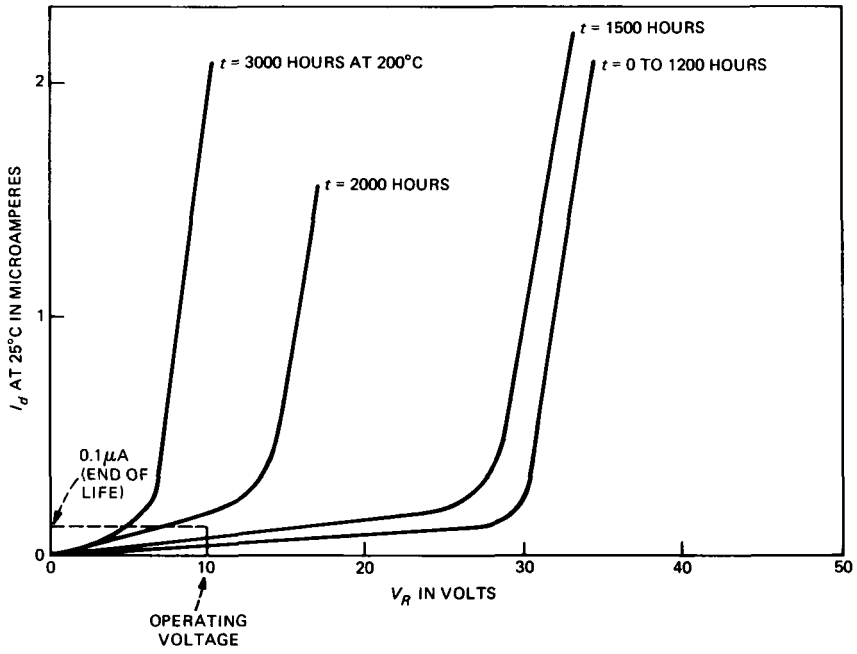

Fig. 2—Typical change in I-V characteristic for photodiodes as a function of aging time.

I_d. Therefore, the devices appear to have a "sudden-failure" characteristic with respect to I_d. A qualitatively similar behavior is observed for silicon photodiodes.[13] Measurements of V_{BR} do not provide an earlier precursor to failure than I_d, and the time to failure is not correlated to the initial value of V_{BR}. In situ measurements of I_d provide, at least for some diodes, an earlier indication of failure than room temperature measurements. The latter is not of significant advantage, however, since failures that occur in several thousand hours (under accelerated conditions) can be identified as impending failures only ~200 hours earlier. Consequently, room temperature measurements are principally used. As indicated previously, it has been found that there are no systematic changes in rise and fall times, quantum efficiency, and capacitance over long-term, high-temperature aging within our experimental error. Increased dark current is therefore the only observed chip-related failure mode.

Figure 3 illustrates several (dark-current) failure distribution plots for receiver photodiodes of early design that were aged at various temperatures. Two modes of failures are observed: early failures of a freak population, which in these devices is a high proportion (0.15) of the sample population; and the main population. At the lowest tem-

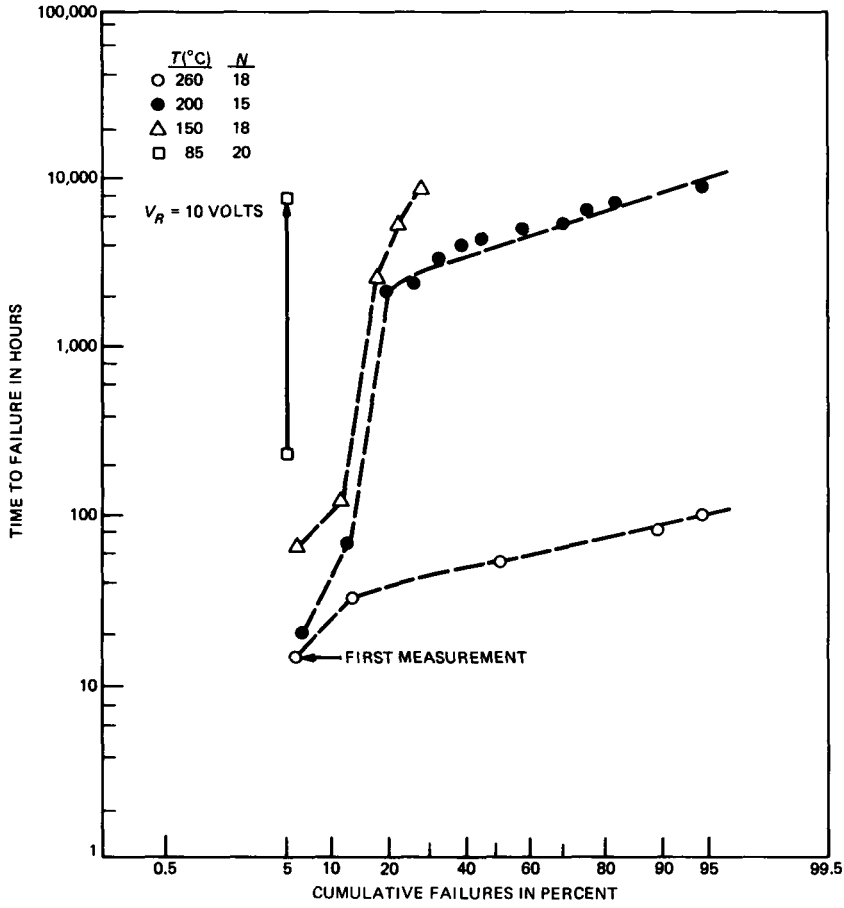

Fig. 3—Dark-current failure distributions for receiver photodiodes of early design after high-temperature aging. The vertical arrow indicates that no further failures have occurred.

peratures ($T < 150$°C), the main population is not clearly defined even after nearly 10^4 hours of aging. In fact, at 85°C the observed changes in I_d (neglecting the first early failure) are within experimental error. The data in Fig. 3 indicate that failures in both the freak and main populations are thermally activated, although not necessarily with the same activation energy. Assuming that the freak population can be removed by some appropriate means (see below), the Median Life (ML) and standard deviation, σ, for the main population can be estimated using conventional censoring techniques.[14]

Figure 4 shows the temperature dependence of ML for 116 receiver photodiodes; the corresponding values of σ are given in parentheses. For 150°C, a worst-case estimate was made assuming that the last

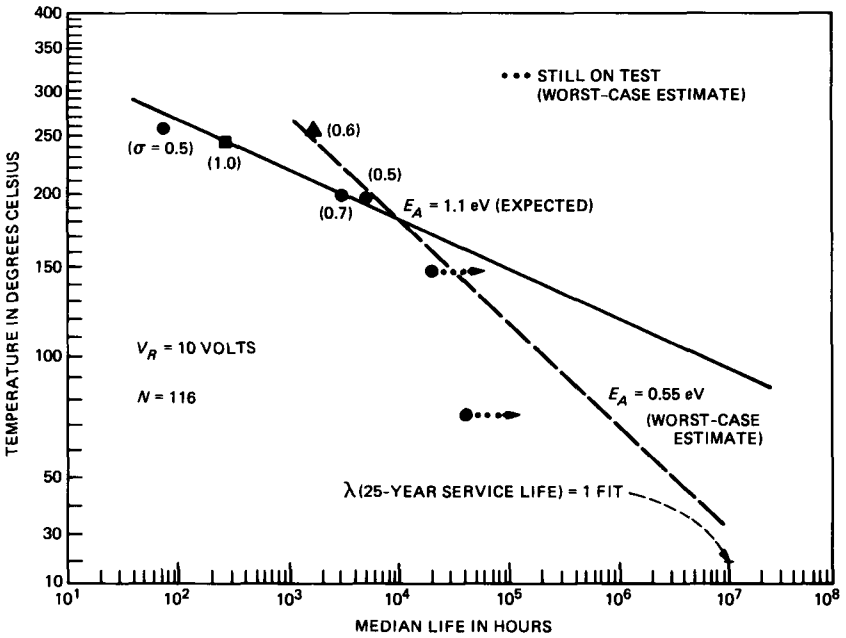

Fig. 4—Median life as a function of temperature for receiver photodiodes. Activation energy estimates vary from 1.1 eV (expected value) to 0.55 eV (worst case). The median life (for $\sigma = 1$) required for a maximum failure rate of 1 FIT over a 25-year service life is shown for reference.

observed failure in the transition region from freak to main population was the first failure of the main population. An average value of $\sigma = 0.8$ was used to extrapolate to ML. In a similar fashion, a worst-case estimate at 85°C indicates ML $\gg 2 \times 10^4$ hrs. Note that at 250 to 260°C there is a spread in estimated values of ML by a factor of ~140. The progressive increase in ML, in fact, reflects systematic improvements in device design and processing. The "probable" activation energy, shown as the dashed line, is 1.1 eV, which is reasonably consistent with the data; a "worst-case" activation energy, shown by the dotted line, is 0.55 eV. On the abscissa is a reference mark at the ML corresponding to a maximum failure rate of 1 FIT over the 25-year service life for TAT-8. The accelerated aging data collected in this phase of the receiver photodiode qualification program predict that even the worst-case estimates are consistent with a 1-FIT reliability objective at SL operating conditions, viz., 10°C undersea and 30°C continental shelf. Similar studies have begun for monitor photodiodes. As these latter devices use identical fabrication technology, operate at a lower bias, and have a higher dark current at end-of-life, it is likely that the 30-FIT reliability objective will be met.

As an adjunct to the above test program, failure mode analysis was

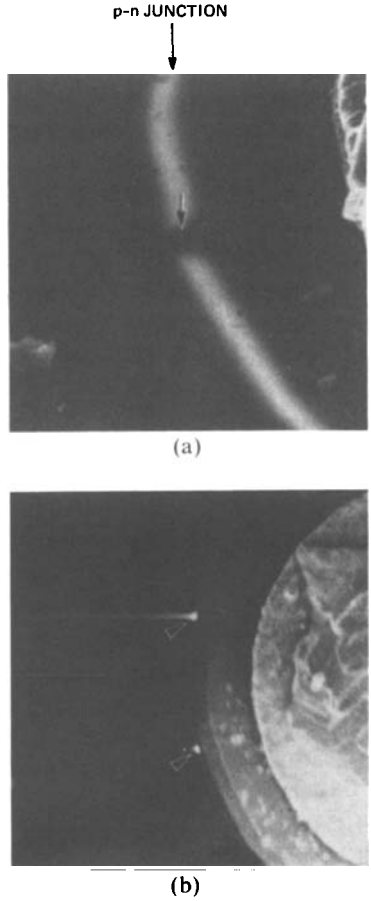

Fig. 5—Electron-beam-induced current signals superimposed on secondary electron images of failed photodiodes. A photodiode with $V_{BR} = 0$ exhibits a leakage path shorting the junction, designated by the arrow in Fig. 5a. A photodiode with a reduced V_{BR} of 8V exhibits localized breakdown, designated by arrows in Fig. 5b, when a reverse bias of 8V is applied.

performed using the Electron-Beam-Induced Current (EBIC) mode of a scanning electron microscope.[15,16] In particular, a correlation was sought between failures and anomalies in the region where the p-n junction intersected the SiN_x passivation layer. For devices for which $V_{BR} = 0$ after aging, a local leakage path shorting the p-n junction is evident, as in Fig. 5a. In other cases, local premature breakdown sites were evident in the EBIC signals when the applied reverse bias was equal to the (reduced) photodiode breakdown voltage, as in Fig. 5b. The cause of the large reduction in V_{BR} is not known but presumably involves the field- and temperature-assisted drift of some impurity species and/or defects to localized sites in the p-n junction. The

localized failure sites have been correlated[16] with microplasmas that are initially present.

4.2 Overvoltage aging at high temperature

To determine the extent to which operating voltage affects reliability, 100 monitor photodiodes were aged at 200°C with reverse bias V_R ranging from 0 to 30V. Figure 6 illustrates the pronounced effect of V_R on ML. It is noted that only I_d failures are observed and no changes in capacitance or quantum efficiency are detected prior to I_d failure. The mode of failure induced by overvoltage is therefore similar to that induced by thermal acceleration. The importance of reverse bias has been previously established in silicon phototransistors where ML was inversely related to V_R.[13] In a device with homogeneous junction characteristics, the leakage current under conditions of high temperature and overvoltage flows uniformly through the junction. Power dissipation is sufficiently low that devices are not impaired. The shortened ML with increased V_R is likely owing to enhanced field-assisted drift of an impurity species to localized sites, as mentioned above. However, if the device is flawed, so that a disproportionally

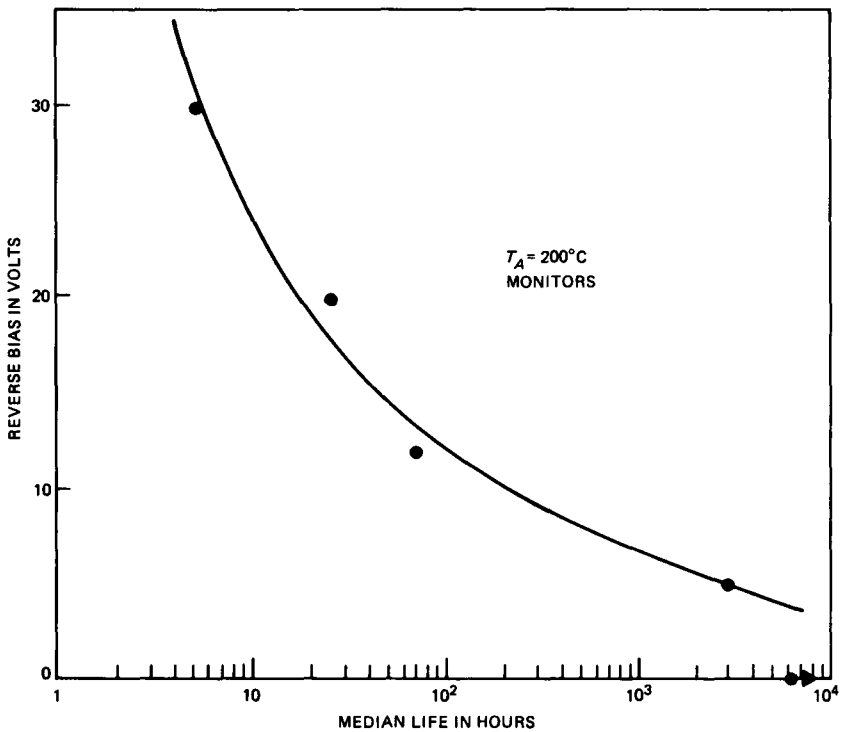

Fig. 6—Effect of reverse bias on the dark-current median life for monitors.

large fraction of the current flows through a small region of the junction, the temperature will rise locally; this will further increase current flow, leading to a runaway process which will ultimately inflict permanent, localized damage, perhaps because of melting or defect generation. At the highest overvoltage, local semiconductor damage was readily visible at the perimeter of the p-n junction.

The previous section showed that temperature at fixed bias accelerates photodiode degradation, while the data presented in Fig. 6 showed that reverse bias at fixed temperature accelerates degradation. Consequently, both parameters can be utilized to formulate an optimum method for purging weak devices. This subject will be treated more fully in Section V.

4.3 Humidity-bias testing

Humidity is known to provide surface leakage paths in reversed-biased diodes, which can ultimately lead to device failure.[13,17] For this reason our photodiodes are hermetically packaged. To assess the sensitivity of the photodiodes to humidity, over 100 unpackaged photodiodes were bias-aged at 85°C with relative humidity levels ranging from <3 to 85 percent.[9] Consistent with studies on other devices[17], ML of I_d failures was reciprocally related to the humidity level, and bias substantially enhanced the degradation rate. However, the mechanism of failure was surprising. Scanning electron microscopy of failed devices revealed that the n-type InGaAs, in the vicinity of the p-n junction, was severely etched. It was postulated that when moisture penetrated the dielectric and bridged the p-n junction, rapid electrochemical oxidation of the n-type semiconductor occurred which damaged the junction, effectively shorting the device. From the humidity data, the critical concentration of moisture at the p-n junction which phenomenologically resulted in device failure was calculated. From the observed time dependence of failure, the corresponding critical ambient moisture level was estimated to be $\sim 3 \times 10^5$ ppm. Consequently, this failure mechanism is eliminated in the hermetic packages used in SL applications, as the entrapped moisture level is $\lesssim$10 ppm.

4.4 Temperature cycling

Initial temperature cycling tests of first-generation photodiodes, which used plated p-contacts, revealed an alarmingly high failure level resulting from wire bond opens. For example, 10 percent of the diodes developed open bonds at the p-contacts after 10 cycles from −55° to 125°C. Bond adherence was substantially improved with the introduction of evaporated contacts. Thus, in 406 receiver photodiodes that were similarly cycled, only two opens developed and no failures developed in 296 monitors. The low incidence of bond failure results from

the fact that the wires are not subject to mechanical constraint in the hermetic packages used here, but it might be the case in a molded or filled package. In the course of this study we found that the thermal cycling can induce significant increases in dark current in ~10 percent of the devices, providing a means of screening out flawed devices. The increase in dark current is presumed to arise from thermally induced stress at the InGaAs-SiN_x interface.

V. PURGE: A MEANS OF ELIMINATING EARLY FAILURES AND IDENTIFYING WEAK DEVICES

It is common with various semiconductor devices to use a high-temperature "burn-in" at the maximum-rated bias to eliminate early failures associated with a freak population of devices in which the failure mechanism is thermally activated. For the burn-in to be effective, the ML of the freak population must be orders of magnitude smaller than the main population, so that the burn-in can be long enough to eliminate (fail) the freak devices without adversely affecting the life of the main population. Figure 3, however, shows that at 200°C, a burn-in of 500 to 1000 hours is needed to eliminate freaks. Such a burn-in is prohibitively long and will significantly shorten the useful life of the remaining devices (ML = 4000 hours). Because of the sudden-failure characteristic, initial degradation rate cannot be used to identify early failures. Finally, a conventional burn-in does not identify flawed devices which may fail by very low activation energy mechanisms.

In Section 3.2, we showed that overvoltage provided a nonthermal means of accelerating photodiode degradation. We have determined that a *combined* stress of high temperature and overvoltage provides an effective purge for failing freak devices and for identifying flawed devices which would likely fail early in the TAT-8 life cycle.[18] Ideally, the purge will result in a population of robust devices that will meet or (more likely) exceed the reliability expected of the main population. To evaluate a trial purge, photodiodes are subjected to a relatively short but strong purge. Weak devices will tend to fail as a result of the purge. For the survivors, the change in I_d provides a useful measure of device stability, which is then used to eliminate additional weak devices. The efficiency of the purge is judged by life testing (high temperature but normal bias) *all* of the survivors and comparing the early failures in the life tests with those identified in the postpurge measurements.

Figure 7 is a histogram of the change in I_d for 33 receiver photodiodes following a 10-hour, 200°C purge at a 2X overvoltage. The purge was sufficient to result in four failures. In general, reverse-bias aging at elevated temperatures results initially in a decrease in I_d, perhaps as

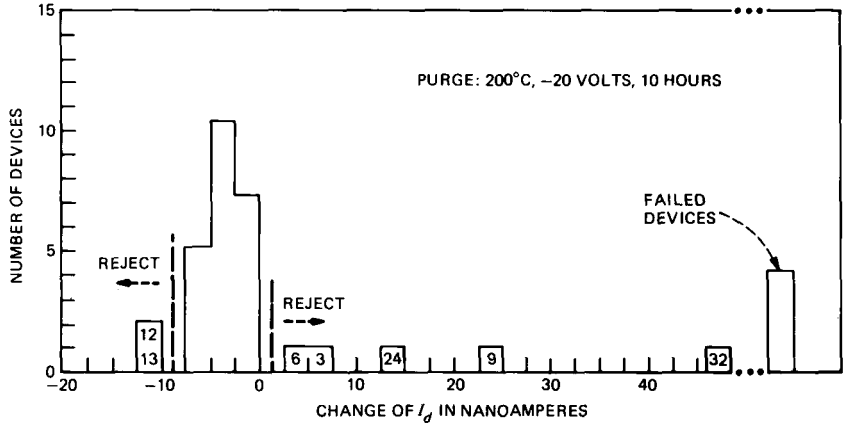

Fig. 7—Histogram of change in I_d for receiver photodiodes following a 200°C purge at 2X overvoltage.

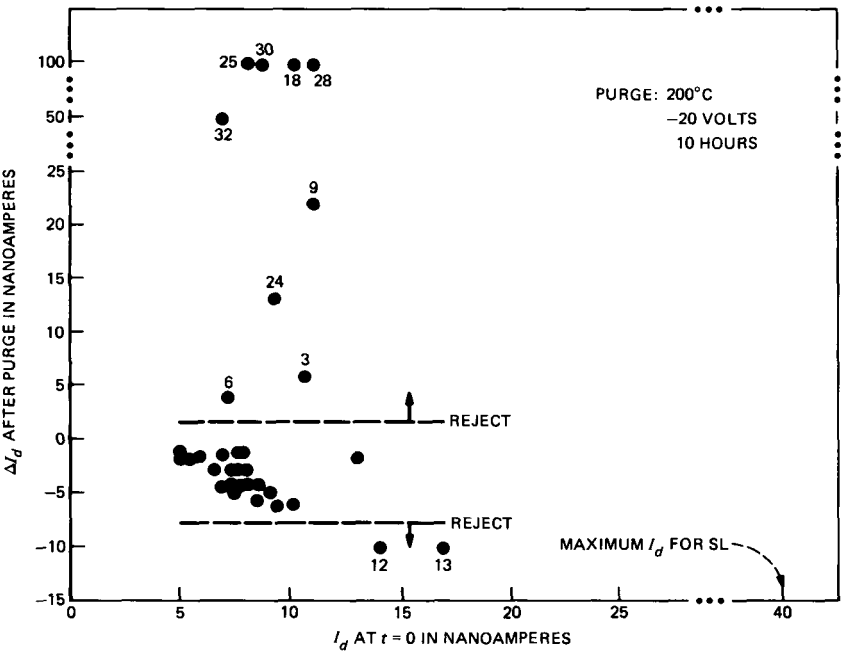

Fig. 8—Change in I_d for receiver photodiodes following a 200°C purge at 2X overvoltage as a function of initial I_d.

a result of stress relief or "stabilization." However, in Fig. 7 we see that several devices show significant increases in I_d, while several others show a higher than nominal reduction in I_d. Large changes in I_d, both positive and negative, are considered to be characteristic of

unstable devices, and consequently those devices should be eliminated. In the histogram these devices are identifed with the device number. Figure 8 shows the change in I_d resulting from the purge as a function of initial I_d. Weak devices, identified in the purge, are indicated with the device number. While there is some tendency for high I_d devices to exhibit the largest change in I_d, there are numerous exceptions. On the other hand, most devices for which I_d is initially greater than 10 nA are culled out in this purge. This result, however, is not general. Consequently, purge yield is not strongly correlated to the initial value of I_d. Similarly, purge yield is not correlated to initial V_{BR}, although devices with very low V_{BR} (<10V) are likely to fail.

Figure 9 shows I_d of the purged population (excluding devices that failed) after 1900 hours of life testing at 200°C and V_R = 10V. The numbered devices are those identified as weak devices in the purge. Note that two of these identified devices failed in the life test, at 310 hours (device 24) and 600 hours (device 32). Also, identified devices 9 and 13 are nearest to failure, i.e., have the highest dark current. Consequently, the purge at 2X overvoltage appears to fail successfully the weakest devices and to identify for removal devices that subsequently fail early. The remaining devices are the most robust portion

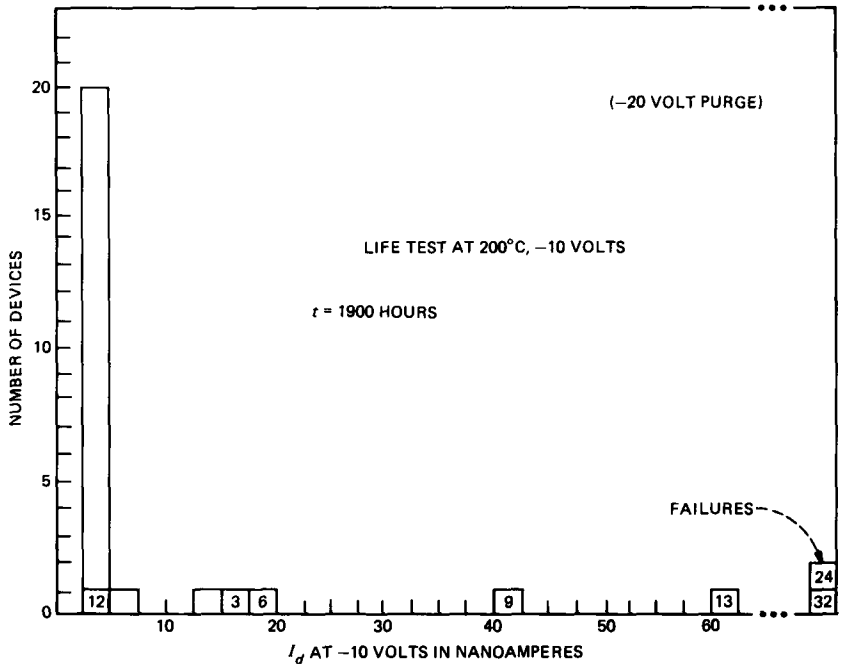

Fig. 9—Histogram of I_d values for the purged devices in Fig. 7 following a 1900-hour life test.

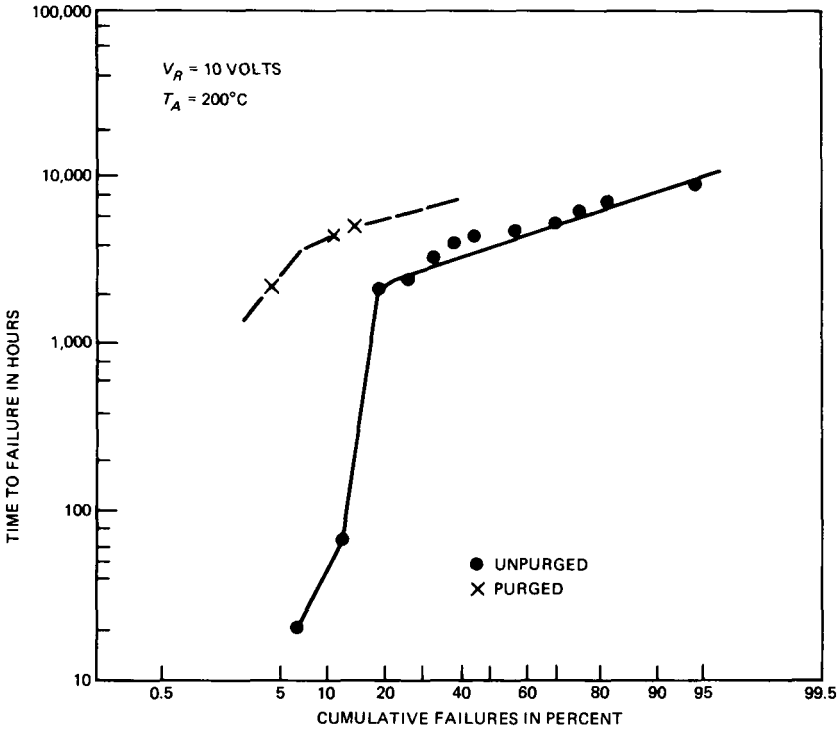

Fig. 10—Dark-current failure distribution for purged and unpurged receiver photodiodes.

of the main population. This is confirmed by Fig. 10, which gives the failure distribution after extended ($7 \cdot 10^3$ hours) life testing of the robust devices (not numbered in Fig. 9) that were identified by the purge. Shown for comparison are unpurged devices. The dramatic reduction in early failures for the purged devices is evident.

One of the drawbacks of the aforementioned trial purge is the lack of wide separation between some of the weak devices and the robust main population. For example, in Fig. 7, devices 12 and 13, and 3 and 6, appear to be part of the tails of the main population. One expects that a purge at higher overvoltage may induce greater changes in I_d in weak devices, thus providing the desired spread. Tests at 3X overvoltage look promising. Figure 11 is a histogram of the change in I_d for receiver photodiodes following purge. Figure 12 is the corresponding histogram of I_d following a subsequent 1800-hour life test. Although the sample size is small, it appears that the stronger purge results in two distinct populations, viz., failed devices and robust devices. Note, for example, comparing Figs. 9 and 12, that after 1800-hour life testing, the purge survivors show less spread in I_d for the stronger purge. In

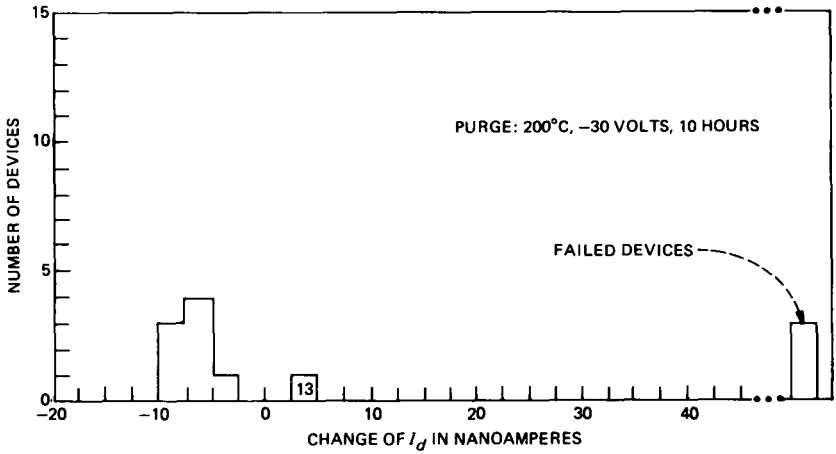

Fig. 11—Histogram of change in I_d for receiver photodiodes following a 200°C purge at 3X overvoltage.

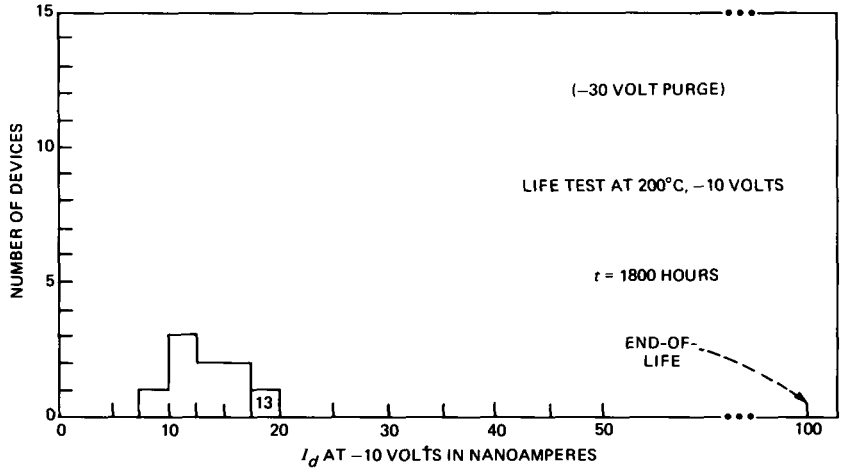

Fig. 12—Histogram of I_d values for the purged devices in Fig. 10 following an 1800-hour life test.

fact, Fig. 13 shows that the change in I_d after the 1800-hour life test is uniformly small for the strong purge, suggesting that the survivors are robust devices.

Additional experiments have been performed to establish optimum purge conditions. Figure 14 summarizes the effect of increased overvoltage, at constant temperature, on receiver photodiode failures. As the overvoltage is increased, the fraction of devices that are failed by

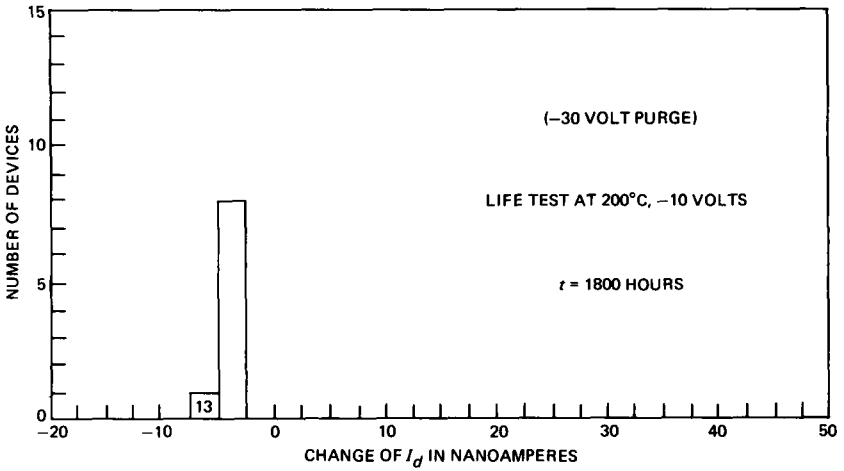

Fig. 13—Histogram of change in I_d for the purged devices in Fig. 10 following an 1800-hour life test.

the purge increases and the fraction of devices that fail a subsequent life test (initially) decreases. However, for the highest overvoltage, the failure level increases rapidly, indicating that "good" devices are being damaged. This is borne out by the corresponding increase in life test failures. Note also the increase in the total (purge plus life test) failure level. The results in Fig. 14 suggest that a 200°C purge at 30V (3X overvoltage) is near optimum for our receiver photodiodes. Similar studies are in progress for monitor photodiodes.

VI. CONCLUSIONS

Testing of planar InGaAs photodiodes under a variety of accelerated conditions reveals that increased dark current is the only detected failure mode. High-temperature aging results to date indicate that, for receiver photodiodes, a device design exists (main population of failures) that is predicted to be consistent with a 1-FIT reliability objective at TAT-8 operating conditions. High reliability (<30 FITs) is expected for monitor photodiodes of similar design. Moreover, a purge using a combination of accelerants (temperature and overvoltage) has been developed, which has considerable promise of eliminating flawed or weak devices that would otherwise fail early in the TAT-8 life cycle. Extended life tests verify that the purge survivors are the most robust devices. Consequently, purge testing coupled with appropriate inspection and thermomechanical screening is expected to provide a means for assuring that the selected devices have a high probability of meeting TAT-8 reliability objectives.

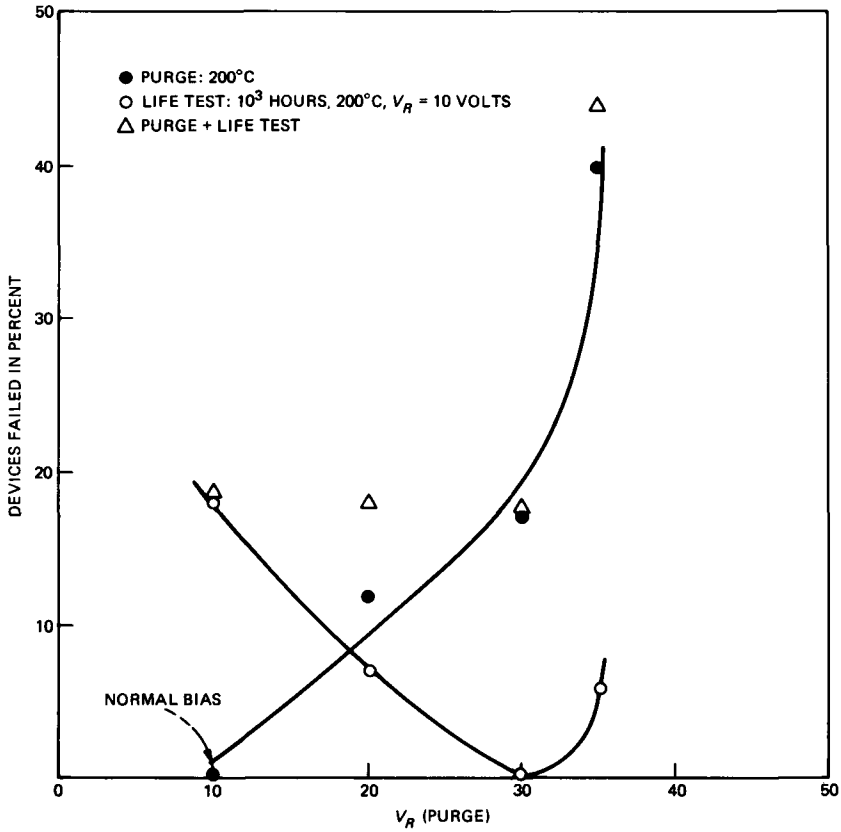

Fig. 14—Effect of reverse bias on resulting receiver photodiode failures for the purge and subsequent life test. Purge time is ten hours except at $V_R = 35$V, for which a time of one hour was used.

VII. ACKNOWLEDGMENTS

It is a pleasure to acknowledge the technical assistance of C. F. King in acquiring the aging data, the cooperation of O. G. Lorimor and W. S. Trimmer in supplying the devices used in these studies, and the encouragement and support of A. A. Bergh. The manuscript has benefited from many useful suggestions of R. L. Hartman and E. I. Gordon.

REFERENCES

1. F. S. Chen, unpublished work.
2. G. H. Olsen and M. Ettenberg, "High Temperature Reliability of Vapor-Grown InGaAs Photodiodes," topical meeting on Optical Fiber Communication, Phoenix, Ariz., April 13–15, 1982.
3. D. G. Jenkins and A. W. Mabbit, "The Reliability of GaInAs Photodiodes and GaAs FETs for Use in PIN-FET Fiber Optic Receivers," IEEE Specialist Conference on Light-Emitting Diodes and Photodetectors, Ottawa-Hull, September 15–16, 1982.

4. J. M. Nemchik and M. J. Buckler, "Design of the *SLC*™ 96 System Loop Lightwave Feature," IEEE Int. Conf. Commun., Boston, Mass., June 1983, Conf. Rec., *I*, pp. 91–4.
5. T. P. Pearsall et al., "A GaInAs/InP Heterophotodiode With Reduced Dark Current," J. Quant. Elec., *QE-17* (February 1981), pp. 255–9.
6. T. P. Lee et al., "Small Area InGaAs/InP p-i-n Photodiodes," Elec. Lett., *16* (February 1980), pp. 155–6.
7. G. H. Olsen, "Low-Leakage, High Efficiency, Reliable VPE InGaAs 1.0–1.7 μm Photodiodes," IEEE Elec. Device Lett., *EDL-2* (September 1981), pp. 217–9.
8. O. G. Lorimor et al., unpublished work.
9. L. S. Lichtmann, P. A. Kohl, and R. H. Burton, "Degradation of Silicon Nitride-Protected InGaAs p-i-n Photodiodes by an Electrochemical Etching Reaction," IEEE Specialist Conference on Light-Emitting Diodes and Photodetectors, Ottawa-Hull, Canada, September 1982.
10. R. H. Saul, "Recent Advances in the Performance and Reliability of InGaAsP LEDs for Lightwave Communication Systems," IEEE Trans. Elec. Devices, *ED-30* (April 1983), pp. 285–95.
11. R. G. Smith and S. D. Personick, *Topics in Applied Physics, 39,* New York, N.Y.: Springer-Verlag, 1980, pp. 89–160.
12. D. P. Schinke, R. G. Smith, and A. R. Hartman, *Topics in Applied Physics, 39,* New York, N.Y.: Springer-Verlag, 1980, pp. 63–87.
13. R. H. Saul et al., unpublished work.
14. D. S. Peck, "The Analysis of Data From Accelerated Stress Tests," Proc. Reliability Phys. Symp., Las Vegas, Nev., March 31, 1971, pp. 69–78.
15. F. S. Chen, P. S. D. Lin, and F. Ermanis, unpublished work.
16. A. K. Chin, F. S. Chen, and F. Ermanis, "Failure Mode Analysis of Planar Zn-Diffused $In_{0.53}Ga_{0.47}As$ PIN Photodiodes," J. Appl. Phys., *55* (March 1984), pp. 1596–606.
17. D. S. Peck and C. H. Zierdt, Jr., "Temperature-Humidity Acceleration of Metal-Electrolysis Failure in Semiconductor Devices," Proc. Reliability Phys. Symp., Las Vegas, Nev., April 3, 1973, pp. 146–52.
18. R. H. Saul and F. S. Chen, "Reliability Assurance for Devices With a Sudden-Failure Characteristic," IEEE Elec. Device Lett., *EDL-4* (December 1983), pp. 467–8.

AUTHORS

Fong S. Chen, B.S. (Electrical Engineering), 1951, National Taiwan University; M.S. (Electrical Engineering), 1955, Purdue University; Ph.D. (Electrical Engineering), 1959, Ohio State University; AT&T Bell Laboratories, 1959—. Mr. Chen has worked on the development of ferrite devices, masers, optical modulators, lightwave transmitters, and on the reliability of photodiodes. He is currently engaged in the development of GaAs integrated circuits. Member, IEEE.

Robert H. Saul, Ph.D (Metallurgy and Materials Science), 1967, Carnegie-Mellon University; AT&T Bell Laboratories, 1967—. Initially, Mr. Saul was engaged in characterization and development of epitaxial growth techniques for opto-electronic materials and devices. In 1972 he became Supervisor of a group responsible for developing visible light-emitting diodes. That work pioneered the use of multislice epitaxial techniques for achieving state of the art performance in a manufacturable growth system. Since 1975 Mr. Saul has supervised a group responsible for developing a variety of infrared light-emitting diodes that are used in optical-isolators and fiber optic systems. His current interests include development of long-wavelength sources for lightwave transmission systems and reliability of detectors. Mr. Saul holds eight patents in the area of materials growth and opto-electronic devices. Senior member, IEEE; member, American Physical Society, Sigma Xi, and Tau Beta Pi. Chairman, 1982 IEEE Specialist Conference on Light-Emitting Diodes and Photodetectors.

Paul W. Shumate, Jr., B.S. (Physics), 1963, College of William and Mary; Ph.D. (Physics), 1968, University of Virginia; Bell Laboratories, 1969–1983. Present affiliation Bell Communications Research, Inc. At Bell Laboratories, Mr. Shumate's work included research on the physical properties of magnetic bubble materials and on memory devices. In 1975 he became Supervisor in the Lightwave Devices and Subsystems Department, where he was subsequently responsible for FT3 laser transmitter development, optical data links for *5ESS*™ switching equipment, laser- and LED-based video transmitters, and p-i-n/FET receivers. Other work included detector packaging and reliability studies for SL, and laser packaging for FT4E. Since transferring to Bell Communications Research in October 1983, where he is District Manager of Lightwave Device Technology, he is responsible for research on very-high-bit-rate digital and heterodyne laser transmitters and receivers. Member, American Physical Society, Phi Beta Kappa, Sigma Xi; Senior Member, IEEE.